Journal of Mechanical Research and Application (JMRA), Vol. 12 No.1, 1401(2022),60-77

Magnetic Hydrodynamic Flow of nanofluid in a square cavity

Jalil. Jamali: Assistant professor- Mechanical engineering Department- Islamic Azad university- South Branch- Tehran- Iran. (Email: jalil.jamali@iau.ac.ir)

Basim Jaber Jwode Alssaray: Msc- - Mechanical engineering Department- Islamic Azad university- South Branch- Tehran- Iran.

Abstract

Purpose – The purpose of this thesis is to study the influence of magnetic field on MHD natural convection flow of hybrid nanofluid in a square cavity with a corrugated conducting block. Also, the effect of fluid–solid thermal conductivity ratio is investigated.

Design, methodology, and approach — The finite volume method is used to discretize the governing equations that are expressed in the dimensionless form. The SIMPLE method ensures the connection of velocity and pressure. The convergence is confirmed using a heat transfer balance. The quantitative and qualitative data were compared with those from other published studies in order to validate the numerical results.

Findings - Based on heat transfer, fluid friction, and magnetic force, the results show that the magnetic field and the conductivity ratio of the wavy solid block can considerably affect the dynamic and thermal field, and, as a result, the rate of heat transfer and entropy generation.

Originality and worth - To the best of the authors' knowledge, this numerical analysis represents the first effort to use hybrid nanofluid for examining the creation of entropy due to magneto hydrodynamic natural convective flow in a square cavity with the presence of a wavelike circular conductive cylinder. The irreversibility caused by the magnetic effect are considered. Consideration is given to the fluid-solid thermal conductivity ratio.

Keywords Entropy generation, Natural convection, Hybrid nanofluid, Magneto-hydrodynamics, Wavy conducting cylinder

INDRODUCTION

1. 1 Background

The convective heat transfer provided by a temperature gradient of an electrically conductive fluid in the presence of a magnetic field, called magnetohydrodynamic (MHD) natural convection, has been the subject of wide attention in the past years. This interest is due to the different applications of such fluids in industry and engineering: purification of molten metals, coolers of nuclear reactors, thermal machines, pumps, valves, MEMs, chemical and biological engineering and solar technology, etc. (Sathiyamoorthy and Chamkha, 2010; Chamkha, 2004).

The structure and intensity of convection heat transfer are directly related to the external thermal solicitations, the nature of the fluid and the geometry of the space where the process takes place. It turns out that the thermal conductivity of non-metallic liquids (water, oil, ethylene glycol) is very low, and that the addition of metallic or metallic oxides nanometric particles which have a higher thermal conductivity in such liquids, therefore called nanofluid, could increase significantly the heat transfer by adjusting the thermal conductivity of the mixture. In this context, several researchers have been interested in the study of the intensification of convection heat transfer using nanofluids as working fluids, such as in references (Izadi *et al.*, 2015; Izadi *et al.*, 2018a; Izadi *et al.*, 2018b; Mehryan *et al.*, 2019a; Izadi *et al.*, 2018c; Izadi *et al.*, 2014).

Hybrid or combined nanofluid is a new category of nanofluids formed by incorporating two kinds of nano-sized particles in ordinary liquids. Choosing of these nanoparticles materials well is also very important. Metallic nanoparticles as Ag, Cu, Al, and Au possess high thermal conductivity, but the use of these nanoparticles is limited due to his low stabilities and high reactivity into base liquids. The uses of metallic oxide nanoparticles such as Al_2O_3, CuO and TiO_2 have multiple beneficial properties as more stability and chemical inertness (Tayebi and Chamkha, 2016; Tayebi and Chamkha, 2017a; Tayebi and Chamkha, 2017b; Mohebbi *et al.*, 2018b).

Many researchers were interested in examining the MHD convective heat transfer in the presence of nanofluid or Hybrid nanofluid, as in very recent investigations mentioned in references (Reddy *et al.*, 2017a; Mehryan *et al.*, 2019b; Reddy *et al.*, 2017b; Izadi *et al.*, 2019a; Reddy *et al.*, 2018; Dogonchi *et al.*, 2019; Rashad *et al.*, 2018; Sajjadi *et al.*, 2019; Izadi *et al.*, 2019b; Izadi *et al.*, 2019c).

In most studies of convection problems, only the first law of thermodynamics (law of conservation of energy) has been used to describe the phenomenon alongside to laws of conservation of mass and momentum. The modern trend in the domain of heat transfer and thermal conception is directed towards the treatment of the second principle of thermodynamics and the resulting concept: the entropy generation that quantifies the energy quality losses caused by irreversibilities that occur in systems (Bejan, 1982; Bejan, 1996).

In particular, there are some few studies that deal with the entropy generation analysis of

MHD convective heat transfer of nanofluids in enclosures. Selimefendigil *et al.* (2016) numerically examined laminar natural convection and entropy generation of nanofluids entrapped in trapezoidal enclosure by using the finite element method. The study is implemented for various values of Hartmann number, Rayleigh number, and nanoparticle volume concentration. Mejri *et al.* (2014) Analyzed the entropy generation due to MHD natural convection flow of a nanofluid filled-square enclosure sinusoidally heated from the side walls. In their work heat transfer and entropy generation due to heat transfer, fluid friction and magnetic force are examined. Abbassi and Orfi (2018) numerically studied MHD natural convection heat transfer in a cavity filled with nanofluids in the presence of a heated element placed on the bottom wall. They reported that the application of magnetic field with an inclination angle of 90° has the highest values of heat transfer coefficient and total irreversibly. A CFD analysis via the finite element method has been performed by Hussain *et al.* (2017) to discuss the entropy generation in MHD mixed convection flow of hybrid nanofluid in an open cavity in the presence of an adiabatic square obstacle. Ghasemi and Siavashi (2017) used the parallel LBM code to numerically study MHD nanofluid natural convection and entropy generation in porous enclosures with different conductivity ratio taking into consideration viscosity-temperature dependence and viscous dissipation. It was found that in smaller and higher values of Rayleigh, heat transfer and fluid friction irreversibilities are respectively dominant, while for moderate values of Rayleigh they have almost the same magnitude. Mansour *et al.* (2017) examined the effect of viscous dissipation on the entropy generation due to MHD natural convection of nanofluid filled-porous square cavity with active parts. Entropy generation and heat transfer of MHD mixed convection flow in a porous enclosure filled with a copper-water nanofluid in the presence of partial slip effect for different values of the influential parameters are examined by Chamkha *et al.* (2017). Malekpour *et al.* (2018a) conducted a numerical study to analyze the second law performance for MHD natural convection in an I-shape cavity filled with copper oxide-water nanofluid. They reported that determining the exact form of the cavity may play an important role in the prediction of heat transfer and entropy generation in the system. Mehryan *et al.* (2018b) have studied the influence of a periodic sinusoidal magnetic field on free convection and entropy generation of ferrofluid continuing in a square cavity.

The presence of solid inner blocks in enclosures may affect the heat transfer and the fluid flow and in turn the entropy generation. The applications of this configuration can be found in solar energy systems, building designs, heat exchangers, and electronic materials. Alsabery *et al.* (2018a) conducted a numerical study to investigate the mixed convective heat transfer in a square enclosure filled with Al_2O_3-water nanofluid in the presence of a solid inner block by using Buongiorno's two-phase model. It was found that the heat transfer rate reduced with the increasing in the size of the block and Richardson number. Zhao *et al.* (2007) examine the influence of a conducting body on the free convection heat transfer inside a square cavity. They found that the thermal conductivity has a great impact on the fluid flow. Mahapatra *et al.* (2013) conducted a numerical study to investigate cooling by natural convection in a square cavity with isothermal and adiabatic bodies. They indicated that the block size much affects the convective heat transfer rate. Sivaraj and Sheremet (2017) considered magnetic field

effects to study free convective heat transfer in a porous inclined square cavity with a heat conducting solid body. Alsabery *et al.* (2018b) have analyzed the second law of thermodynamics and convective heat transfer in a wavy porous cavity including a solid conductive rotating cylinder. Izadi *et al.* (2019d) have made a numerical study using the finite volume method to investigate mixed convection of a nanofluid in a 3D rectangular channel. Effect of opposed buoyancy force on thermohydrodynamic parameters and entropy generation is examined. Alsabery *et al.* (2018c) have investigated numerically the impact of a conducting solid body on natural convection within a square cavity heated on the corner using the two-phase nanofluid model. They reported that the rising of the body thermal conductivity at a fixed size improves the heat transfer rate when the convection is weak. Garoosi and Rashidi (2017) studied conjugate free convection in a heat exchanger comprising various conducting blocks using the two-phase nanofluid model. They reported that the heat transfer rate was considerably affected by varying the orientation of the conductive partition from vertical to horizontal mode. Alsabery *et al.* (2018d) studied the problem of MHD natural convection of alumina water-based nanofluid in a square enclosure having a conducting inner block using the two-phase nanofluid model. As results, they indicated that the influence of the nanoparticles concentration on the Nusselt number is considerable at low Rayleigh, large Hartmann and large values of the block size when the conduction heat transfer is dominated.
Motivated by the citations mentioned above, the present numerical study is a first attempt to use hybrid water-based suspension of Al_2O_3 and Cu nanoparticles for study the entropy generation due to MHD natural convective flow in a square cavity with the presence of a wavy circular conductive cylinder. The influence of the Brownian motion is considered in determining the hybrid nanofluid properties. Hydrodynamic characteristics and heat transfer, as well as the entropy generation are examined for different volume fractions, Rayleigh number, Hartmann number and ratio fluid to solid thermal conductivities at constant values of size, undulation number and undulation amplitude of the wavy cylindrical body. This configuration has many practical industrial and engineering applications, such as in solar thermal collector's design, thermal building design, air conditioning, cooling of electronic elements and nuclear reactors, chemical processing equipment, drying technology, lubrication and furnaces, etc.

3. Mathematical Modeling

In a square cavity containing a wavy cylindrical body, a Cu-Al2O3/water hybrid nanofluid is naturally convection in a constant 2D magneto-hydrodynamic process, as shown in Figure 1. A hot left wall and a cool right wall have a differential in temperature that causes free convection to flow. The horizontal bottom and top walls are adiabatic. For this particular range of Rayleigh numbers, we acknowledge that the hybrid nanofluid flow is incompressible and laminar. Al2O3 and Cu nanoparticles are mixed together and dispersed in host

water to create the hybrid nanofluid. Concentrations of hybrid nanoparticles in volume, f, are equal to 0, 3, 6, and 9%. For the host fluid, the Prandtl value is 6.2.

The wall shape of the wavy inner circular block corresponds to the following equation:

$$r(\eta) = r + \left(Acos(N\eta)\right) \quad (1)$$

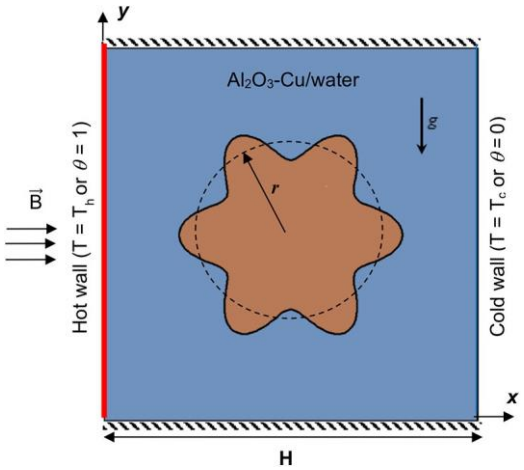

Figure1: Physical model and boundary conditions

where r is the base circle radius, N&A are undulation number & the amplitude, respectively and h is the angular position around the block wall.

In this present configuration, the undulations number, N and its amplitude, A as well as the block size are kept constant corresponding to 6, 0.2 and 2r/H = 0.5, respectively.

The thermophysical properties of the working nanofluid are supposed constant, except for density, which is varied depending on the Boussinesq model. The reference temperature for the Boussinesq approximation is Tc. Thermal equilibrium is assumed between the host liquid and the nano-sized particles. The thermophysical properties of the solid nanoparticles and regular water are exhibited in Table 1

The hybrid nanofluid effective density is.

$$\rho_{hnf} = \left(1 - \emptyset_{Cu} - \emptyset_{Al_2O_3}\right)\rho_f + \rho_{Cu}\emptyset_{Cu} + \rho_{Al_2O_3}\emptyset_{Al_2O_3} \quad (2)$$

The hybrid nanofluid heat capacitance is expressed as:

$$(\rho Cp)_{hnf} = \left(1 - \emptyset_{Cu} - \emptyset_{Al_2O_3}\right)(\rho Cp)_f + (\rho Cp)_{Cu}\emptyset_{Cu} + (\rho Cp)_{Al_2O_3}\emptyset_{Al_2O_3} \quad (3)$$

The hybrid nanofluid effective thermal expansion coefficient is defined as.

$$(\rho\beta)_{hnf} = \left(1 - \emptyset_{Cu} - \emptyset_{Al_2O_3}\right)(\rho\beta)_f + (\rho\beta)_{Cu}\emptyset_{Cu} + (\rho\beta)_{Al_2O_3}\emptyset_{Al_2O_3} \quad (4)$$

The hybrid nanofluid effective dynamic viscosity for 30nm partical-size (dρ) can be calculated using Corcione correlation (Corcione,2011) as.

$$\mu_{hnf} = \mu_f/(1 - 34.87(d\rho/df)^{-0.3}(\emptyset_{Cu} + \emptyset_{Al2o3})^{1.03}) \quad (5)$$

Where the diameter of the water molecule equal to df=3.85×$10^{-10}m$ (Corcione,2011).

The effective thermal conductivity of the hybrid nanofluid is calculated according to the Corcione correlation (Corcione,2011).

$$k_{hnf} = k_f(1 + 4.4Re^{0.4}Pr^{0.66}\left(\frac{T}{T_{fr}}\right)^{10}\left(\frac{k_p}{k_f}\right)^{0.03}(\emptyset_{Cu} + \emptyset_{Al2o3})^{0.66}) \quad (6)$$

Where the nanoparticle Reynolds number, Re is determined as.

$$\text{Re}=2k_b\rho_f T/\pi{\mu_f}^2 d_p \quad (7)$$

The electrical effective conductivity is defined by Maxwell (Maxwell,1881).

Table 1: The base fluid's and the nanoparticles' thermophysical characteristics (Mansour et al., 2016)

Material	$Cp(J.Kg^1K^{-1}$	$\rho(Kg.m^{-3})$	$k(W.m^1K^{-1})$	$\sigma(Sm^{-1})$	$\beta(K^{-1})$
Water	4,179	997.1	0.613	0.05	21×10^{-5}
Cu	385	8,933	401	5.96×10^7	1.67×10^{-5}
Al_2O_3	765	3,970	40	1×10^{-10}	0.85 × 10^{-5}

$$\sigma_{hnf} = \sigma_f(1 + 3\left(\frac{\sigma_{hp}}{\sigma_f} - 1\right)(\emptyset_{Al_2O_3} + \emptyset_{Cu})/-\left(\frac{\sigma_{hp}}{\sigma_f} - 1\right)(\emptyset_{Al_2O_3} + \emptyset_{Cu})) \quad (8)$$

Where

$$\sigma_{hp} = (\emptyset_{Al_2O_3}\sigma_{Al_2O_3} + \emptyset_{Cu}\sigma_{Cu})/(\emptyset_{Al_2O_3} + \emptyset_{Cu})$$

Partial differential equations (PDEs) are created for this problem's description while taking the following premises into consideration (Selimefendigil et al., 2016; Mejri et al., 2014; Mansour et al.,2017).

3.1 Continuity equation

$$\frac{\partial u}{\partial x}+\frac{\partial v}{\partial y}=0 \qquad (9)$$

3.2 Navier-Stokes

$$u\frac{\partial u}{\partial x}+v\frac{\partial u}{\partial y}=-\frac{1}{\rho_{hnf}}\frac{\partial p}{\partial x}+\frac{\mu_{hnf}}{\rho_{hnf}}\left(\frac{\partial^2 u}{\partial x^2}+\frac{\partial^2 u}{\partial y^2}\right) \qquad (10a)$$

$$u\frac{\partial v}{\partial x}+v\frac{\partial v}{\partial y}=-\frac{1}{\rho_{hnf}}\frac{\partial p}{\partial y}+\frac{\mu_{hnf}}{\rho_{hnf}}\left(\frac{\partial^2 v}{\partial x^2}+\frac{\partial^2 v}{\partial y^2}\right)+\frac{(\rho\beta)_{hnf}}{\rho_{hnf}}g(T-T_c)-\frac{\sigma_{hnf}}{\rho_{hnf}}B^2{}_0 v \qquad (10b)$$

3.3 Energy equation for hybrid nanofluid flow.

$$u\frac{\partial T}{\partial x}+v\frac{\partial T}{\partial y}=\alpha_{hnf}\left(\frac{\partial^2 T}{\partial x^2}+\frac{\partial^2 T}{\partial y^2}\right) \qquad (11a)$$

3.4 Energy equation for the conducting solid block.

$$\frac{\partial\left(k_s\frac{\partial T}{\partial x}\right)}{\partial x}+\frac{\partial\left(k_s\frac{\partial T}{\partial y}\right)}{\partial y}=0 \qquad (11b)$$

3.5 Entropy generation equation.

The irreversibilities resulting from heat transfer (slht), fluid friction (slfr), and magnetic field effect (slm) are what lead to the formation of dimensional local total entropy (slt), which is represented by the following equations (25, 26).

$$S_{lt}=\frac{k_{hnf}}{T_{ref}2}\left[\left(\frac{\partial T}{\partial x}\right)^2+\left(\frac{\partial T}{\partial y}\right)^2\right]+\frac{\mu_{hnf}}{T_{ref}}\left[2\left(\frac{\partial u}{\partial x}\right)^2+2\left(\frac{\partial v}{\partial y}\right)^2+\left(\frac{\partial v}{\partial x}+\frac{\partial u}{\partial y}\right)^2\right]+\frac{\sigma_{hnf}}{T_{ref}}B^{2}{}_0 v^2 \qquad (12)$$

$$S_{lt}=S_{lht}+S_{lfr}+S_{lm} \qquad (13)$$

Where

$$T_{ref} = \frac{T_h + T_c}{2}$$

The following characteristic variables are introduced.

$$X = \frac{x}{H}, Y = \frac{y}{H}, U = \frac{H}{\alpha_f}u, V = \frac{H}{\alpha_f}v, P = \frac{pH^2}{\rho_{hnf}\alpha_f 2}, \theta = \frac{T - T_c}{T_h - T_c}, k^* = \frac{k_f}{k_s}$$

$$S_{lt} = S_{lt}\frac{\left(T_{ref}H\right)^2}{k_f(T_h - T_c)^2}$$

The dimensionless governing equations, as follows.

$$\frac{\partial U}{\partial x} + \frac{\partial V}{\partial y} = 0 \qquad (14)$$

$$U\frac{\partial U}{\partial X} + V\frac{\partial U}{\partial Y} = -\frac{\partial P}{\partial Y} + \frac{\mu_{hnf}}{\alpha_f\alpha_{hnf}}\left(\frac{\partial^2 U}{\partial X^2} + \frac{\partial^2 U}{\partial Y^2}\right) \qquad (15a)$$

$$U\frac{\partial V}{\partial X} + V\frac{\partial V}{\partial Y} = -\frac{\partial P}{\partial Y} + \frac{\mu_{hnf}}{\alpha_f\alpha_{hnf}}\left(\frac{\partial^2 V}{\partial X^2} + \frac{\partial^2 V}{\partial Y^2}\right) + \frac{(\rho\beta)_{hnf}}{\rho_{hnf}\beta_f}RaPr\theta$$

$$-\frac{\rho_f}{\rho_{hnf}}\frac{\rho_{hnf}}{\rho_f}Ha^2PrV \qquad (15b)$$

$$U\frac{\partial \theta}{\partial x} + V\frac{\partial \theta}{\partial y} = \frac{\alpha_{hnf}}{\alpha_f}\left(\frac{\partial^2 \theta}{\partial x^2} + \frac{\partial^2 \theta}{\partial y^2}\right) \qquad (16)$$

$$\frac{\partial\left(k^*\frac{\partial\theta}{\partial X}\right)}{\partial X} + \frac{\partial\left(k^*\frac{\partial\theta}{\partial Y}\right)}{\partial Y} = 0 \qquad (17)$$

$$S_{lt} = \frac{k_{hnf}}{T_{ref}2}\left[\left(\frac{\partial\theta}{\partial X}\right)^2 + \left(\frac{\partial\theta}{\partial Y}\right)^2\right]$$

$$+\frac{\mu_{hnf}}{\mu_f}x\left[2\left(\frac{\partial U}{\partial X}\right)^2 + 2\left(\frac{\partial V}{\partial Y}\right)^2 + \left(\frac{\partial V}{\partial X} + \frac{\partial U}{\partial Y}\right)^2\right] + \frac{\sigma_{hnf}}{\sigma_f}xH_a2V^2 \qquad (18)$$

$$S_{lt} = S_{lfr} + S_{lht} + S_{lm} \qquad (19)$$

Where x is the irreversibility factor, which is given as follows:

$$x = \frac{\mu_f a f^2 T_{ref}}{k_f H^2 (T_h - T_c)^2}$$

The total entropy generation averaged on the total volume of the studied geometry is:

$$S_T = \frac{1}{V}\int S_{lt} dV \qquad (20)$$

$$S_T = S_{HT} + S_{Fr} + S_M \qquad (21)$$

Stream function is defined as:

$$U = \frac{\partial \psi}{\partial Y}, V = \frac{\partial \psi}{\partial X} \qquad (22)$$

The non-dimension number coming in the preceding equations are determined as :

$$Ra = \frac{g(T_h - T_c)\beta_f H^3}{v_f \alpha_f}, Pr = \frac{v_f}{\alpha_f}, H_a = HB_0\sqrt{\frac{\sigma_f}{\mu_f}}$$

The dimensionless boundary conditions are written as:

Left wall (X=0, 0≤Y≤1):U=V=0,$\theta = 1$

Right wall (X=1,0≤Y≤1):V=0,$\theta = 0$

Adiabatic walls (Y=0,Y=1,0≤X≤1):U=V=0,$\frac{\partial \theta}{\partial Y} = 0$

Solid-nanofluid interfaces of solid block : U=V=0, $\theta_{hnf} = \theta_s$,$k^*(\frac{\partial \theta}{\partial n})_{hnf} = (\frac{\partial \theta}{\partial n})_s$ (23)

Calculation of the local Nusselt number on the left heated wall is performed as:

$$Nu = \left(-\frac{k_{hnf}}{k_f}\right)\frac{\partial \theta}{\partial X} \qquad (24)$$

The mean Nusselt number is calculated as:

$$Nu_{avg} = \int_0^1 NudY \tag{25}$$

Local Bejan number is expressed as:

$$Be_l = \frac{S_{lht}}{S_{lt}} \tag{26}$$

The average Bejan number (Be_{avg}) is calculated as:

$$Be_{avg} = \frac{1}{V}\int Be_l dV \tag{27}$$

3.3. Numerical procedures

The above dimensionless governing equations [equation (14)-(19)] with associated dimensionless boundary conditions [equation (23)] were numerically discretized using the finite volume method developed by Patankar (1980). The second order upwind scheme was applied for discretization of the diffusive and convective terms. The SIMPLER algorithm has been applied for the velocity–pressure coupling which is an extensively used and well-served algorithm in fluid flow calculations. The resulting algebraic equations systems are solved using the sweeping (line by line [LBL]) method. The convergence criteria for all dependent variables is 10^{-5}. Other tests were carried out by performing an energy balance. In fact, as the horizontal walls are adiabatic, all the energy that is generated in the cavity through the hot left wall must come out through the cold right wall. This energy balance has been verified at 1 per cent.

To evaluate the influence of the grid size on the results obtained, the problem was solved numerically by considering different grid sizes. Table II shows the variation of Nusselt number on the hot wall according to the number of nodes in the grid for the case of Ra = 10^5, Ha = 25, k* = 0.1, and f = 0.06. According to the table, we retain the mesh (121 121) for the rest of the calculations which ensures a mesh-independent solution.

The most important point is to check the accuracy of the results obtained. For this purpose, the adopted model has been validated by performing calculations on the configuration presented by House *et al.* (1990) and by Ilis *et al.* (2008). The results were in good agreement with the corresponding results as shown in Figures 2-5 and Table III.

Table II.Grid independence test mean Nusselt numbers for Ra=10^5 ,Ha=25 ,k^*=0.1 ,and $\emptyset = 0.06$

Grid size	41x41	61x61	81x81	101x101	121x121	141x141
Nu_{avg}	5.129	4.345	3.954	3.893	3.864	3.861

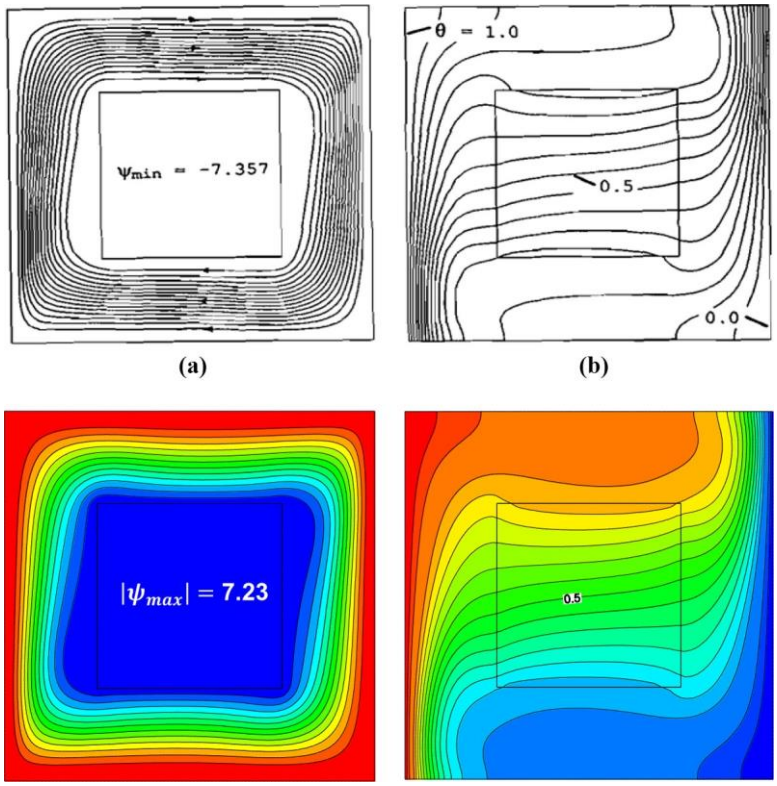

Figure 2. Comparison of isotherms and streamlines with House et al. (1990) for k*=5 and Ra = 10^5

Conclusion

The issue of entropy generation for convective heat transfer of a Cu-Al_2O_3 /water hybrid nanofluid in a square enclosure while taking into account a wavy circular conducting cylinder and magnetic field is numerically analyzed in this paper. Statistical outcomes have been attained for

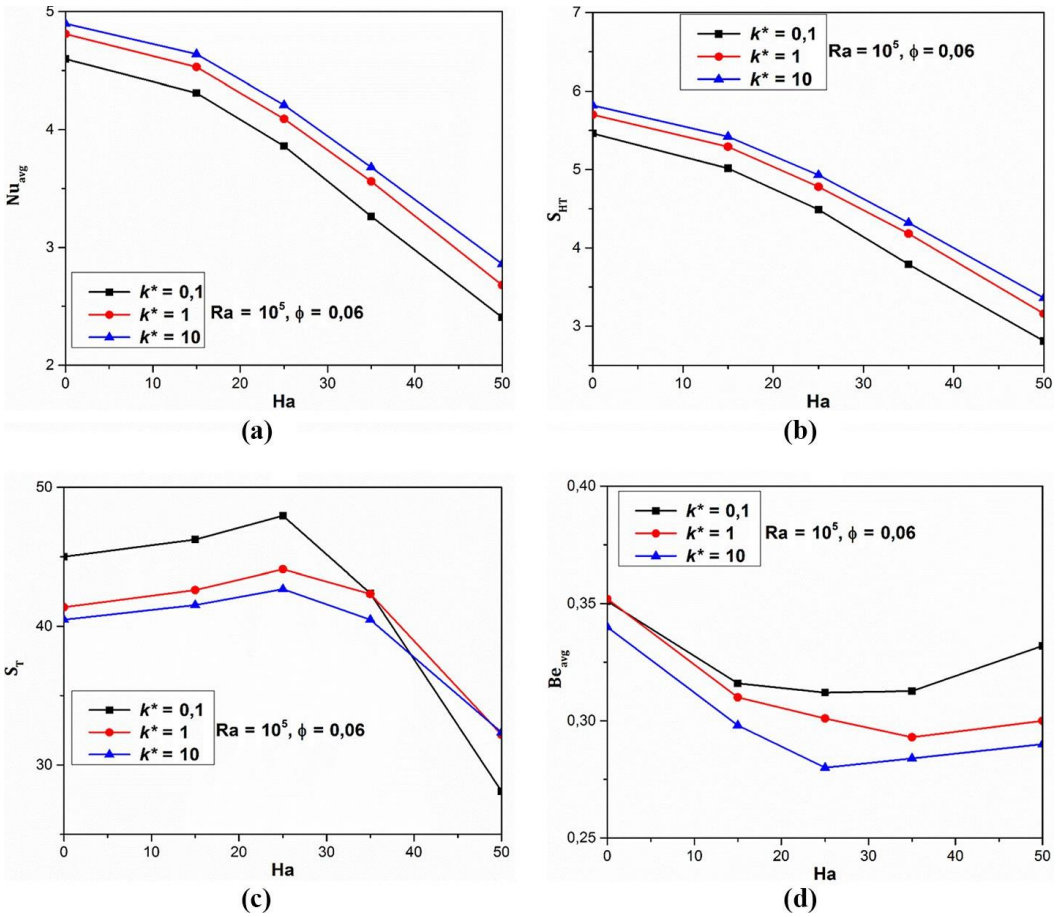

Figure 9.

Variation of (a) Nu_{avg}, (b)entropy generation due to heat transfer, (c) total entropy generation and (d) Be_{avg} with Hartman number for different values of k^*

several values of the Rayleigh number, Al_2O_3-Cu hybrid nanoparticles volumetric fraction, Hartmann number, fluid to solid thermal conductivity ratio. The size of the wavy cylinder, undulation number of the corrugated wall and its amplitudes are kept constant. The principal conclusions of this investigation are as follows:

- The flow circulation is intensified when Hartmann number and thermal conductivity ratio were increased.
- Increasing buoyancy forces causes the entropy generation due to heat transfer, fluid flow, magnetic effects as well as the total entropy generation to increase and average Bejan number to decreases.

- When conduction is the dominant mechanism of heat transfer, elevating the thermal conductivity ratio reduces the heat transfer rate and heat transfer irreversibility.
- The conductivity ratio effect is more considerable on heat transfer rate and heat transfer irreversibility at low Rayleigh and on average Bejan number at moderate Rayleigh.
- When the convection is strong, regardless Hartmann number, an increase in the conductivity ratio leads to an increase in Nusselt number and heat transfer irreversibility, but to a decrease in the total irreversibility and average Bejan number
- Heat transfer rate and heat transfer entropy generation decreased as the Hartmann number was increased, while, the total entropy produced within the cavity shows maximum values corresponding to minimum values of average Bejan number for optimal values of the Hartmann number for each value of thermal conductivity ratio.
- The presence of hybrid nanoparticles in the water was improved the heat transfer rate, irreversibility due to heat transfer, fluid flow, and magnetic effects as well as total entropy generation while it does not affect average Bejan number.

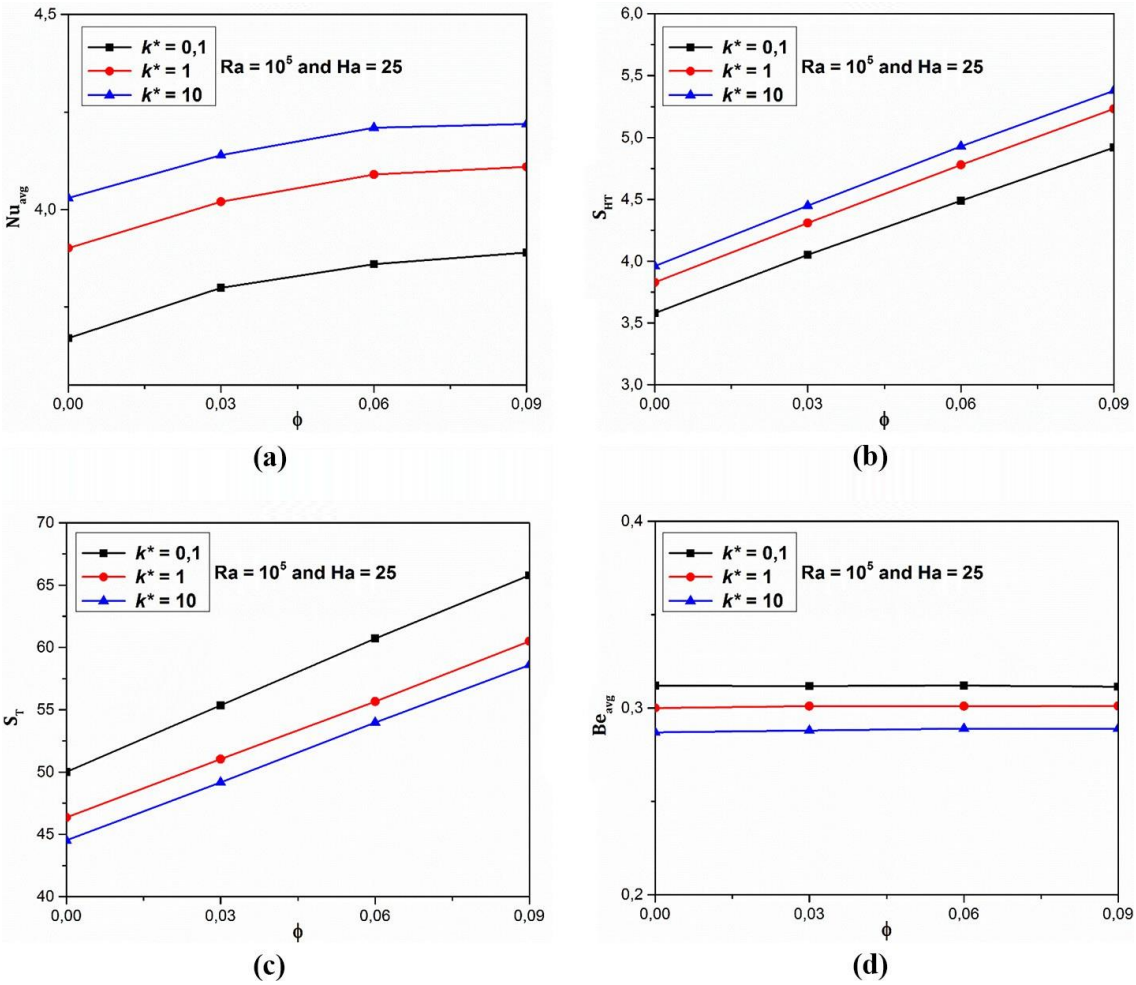

Figure 10.

Variation of (a) Nu_{avg}, (b) entropy generation due to heat transfer, (c) total entropy generation and (d) Be_{avg} with volume fraction for different values

References

[1] Baïri A. Thermal design of tilted electronic assembly with active QFN16 package subjected to natural convection. Int Commun Heat Mass Transf 2015;66:240e5.

[2] Bhowmik H, Tou K. Experimental study of transient natural convection heat transfer from simulated electronic chips. Exp Therm Fluid Sci 2005;29: 485e92.

[3] Oztop HF, Estell € e P, Yan W, Al-Salem K, Or fi J, Mahian O. A brief review of natural convection in enclosures under localized heating with and without nanofluids. Int Commun Heat Mass Transf 2015;60:37e44.

[4] Ju arez JO, Hinojosa JF, Xaman JP, Tello MP. Numerical study of natural convection in an open cavity considering temperature-dependent fluid properties. Int J Therm Sci 2011;50:2184e97.

[5] Suarez MJ, Sanjuan C, Guti errez AJ, Pistono J, Blanco E. Energy evaluation of an horizontal open joint ventilated façade. Appl Therm Eng 2012;37:302e13.

[6] Xam an J, Tun J, Alvarez G, Chavez Y, Noh F. Optimum ventilation based on the overall ventilation effectiveness for temperature distribution in ventilated cavities. Int J Therm Sci 2009;48:1574e85.

[7] Baïri A. Transient natural 2D convection in a cylindrical cavity with the upper face cooled by thermoelectric peltier effect following an exponential law. Appl

Therm Eng 2003;23:431e47.

[8] Edwards D, Catton I. Prediction of heat transfer by natural convection in

closed cylinders heated from below. Int J Heat Mass Transf 1969;12:23e30.

[9] Huang D, Hsieh S. Analysis of natural convection in a cylindrical enclosure.

Numer Heat Transf Part A Appl 1987;12:121e35.

[10] Basak T, Roy S, Thirumalesha C. Finite element analysis of natural convection

in a triangular enclosure: effects of various thermal boundary conditions.

Chem Eng Sci 2007;62:2623e40.

[11] Akinsete VA, Coleman T. Heat transfer by steady laminar free convection in

triangular enclosures. Int J Heat Mass Transf 1982;25:991e8.

[12] Karyakin YE, Sokovishin YA, Martynenko O. Transient natural convection in

triangular enclosures. Int J Heat Mass Transf 1988;31:1759e66.

[13] Shiina Y, Fujimura K, Kunugi T, Akino N. Natural convection in a hemispherical

enclosure heated from below. Int J Heat Mass Transf 1994;37:1605e17.

[14] Baïri A, de María JG. Numerical and experimental study of steady state free

convection generated by constant heat flux in tilted hemispherical cavities. Int

J Heat Mass Transf 2013;66:355e65.

[15] de Vahl Davis G, Jones I. Natural convection in a square cavity: a comparison

exercise. Int J Numer Methods Fluids 1983;3:227e48.

[16] Saitoh T, Hirose K. High-accuracy bench mark solutions to natural convection

in a square cavity. Comput Mech 1989;4:417e27.

[17] Hortmann M, Peric M, Scheuerer G. Finite volume multigrid prediction of

laminar natural convection: bench-mark solutions. Int J Numer Methods

Fluids 1990;11:189e207.

[18] Huelsz G, Rechtman R. Heat transfer due to natural convection in an inclined

square cavity using the lattice boltzmann equation method. Int J Therm Sci

2013;65:111e9.

[19] Leal M, Perez-Guerrero J, Cotta R. Natural convection inside two-dimensional

cavities: the integral transform method. Commun Numer Methods Eng

1999;15:113e25.

[20] Baïri A, Zarco-Pernia E, De María J-MG. A review on natural convection in

enclosures for engineering applications. the particular case of the parallelogrammic diode cavity. Appl Therm Eng 2014;63:304e22.

[21] Hussein AK, AWAD MM, Kolsi L, Fathinia F, Adegun I. A comprehensive review

of transient natural convection flow in enclosures. J Basic Appl Sci Res 2014;4

[22] Patterson J, Imberger J. Unsteady natural convection in a rectangular cavity.
J Fluid Mech 1980;100:65e86.
[23] Hyun JM, Lee JW. Numerical solutions for transient natural convection in a square cavity with different sidewall temperatures. Int J Heat Fluid Flow 1989;10:146e51.
[24] Krishna Satya Sai B, Seetharamu K, Aswatha Narayana P. Solution of transient

laminar natural convection in a square cavity by an explicit finite element scheme. Numer Heat Transf 1994;25:593e609.
[25] Christon MA, Gresho PM, Sutton SB. Computational predictability of timedependent natural convection flows in enclosures (including a benchmark solution). Int J Numer Methods Fluids 2002;40:953e80.
[26] Samanes J, García-Barberena J, Zaversky F. Modeling solar cavity receivers: a
review and comparison of natural convection heat loss correlations. Energy Procedia 2015;69:543e52.
[27] Le Quer e P, Weisman C, Paill ere H, Vierendeels J, Dick E, Becker R, Braack M,
Locke J. Modelling of natural convection flows with large temperature differences: a benchmark problem for low mach number solvers. part 1. reference solutions. ESAIM Math Model Numer Anal. 2005;39:609e16.
[28] Gray DD, Giorgini A. The validity of the boussinesq approximation for liquids
and gases. Int J Heat Mass Transf 1976;19:545e51.
[29] Spradley L, Churchill S. Pressure-and buoyancy-driven thermal convection in
a rectangular enclosure. J Fluid Mech 1975;70:705e20.
[30] Zhong Z, Yang K, Lloyd J. Variable property effects in laminar natural convection in a square enclosure. J Heat Transf 1985;107:133e8.
[31] Sehyun S, Cho YI, Gringrich WK, Shyy W. Numerical study of laminar heat transfer with temperature dependent fluid viscosity in a 2:1 rectangular duct. Int J Heat Mass Transf 1993;36:4365e73.
[32] Xie C, Hartnett J. Influence of variable viscosity of mineral oil on laminar heat
transfer in a 2:1 rectangular duct. Int J Heat Mass Transf 1992;35:641e8.
[33] Leal M, Machado H, Cotta R. Integral transform solutions of transient natural
convection in enclosures with variable fluid properties. Int J Heat Mass Transf 2000;43:3977e90.
[34] Sun H, Lauriat G, Sun D, Tao W. Transient double-diffusive convection in an
enclosure with large density variations. Int J Heat Mass Transf 2010;53: 615e25.
[35] Quer e L. Accurate solutions to the square differentially heated cavity at high
rayleigh number. Comput Fluids 1991;20:2941.
[36] Lemmon EW, Jacobsen RT, Penoncello SG, Friend DG. Thermodynamic

properties of air and mixtures of nitrogen, argon, and oxygen from 60 to 2000 k at
pressures to 2000 mpa. J Phys Chem Ref. data 2000;29(3):331e85.